

Relaxation processes in the ferroelectric and alpha phases of antiferroelectric liquid crystals

F. Bibonne¹, J.P. Parneix^{1,a}, and H.T. Nguyen²

¹ Laboratoire de Physique des Interactions Ondes-Matière^b, ENSCPB, avenue Pey-Berland, BP 108, 33402 Talence Cedex, France

² Centre de Recherche Paul Pascal^c, avenue A. Schweitzer, 33600 Pessac Cedex, France

Received: 24 February 1998 / Revised: 11 May 1998 / Accepted: 26 May 1998

Abstract. Dielectric measurements of a new antiferroelectric liquid crystal series exhibiting different phase sequences have been carried out as a function of frequency from 10 Hz to 10 MHz. Structural properties of $S_{C_\alpha}^*$ and ferroelectric $S_{C_{FI}}^*$ phases were discussed on the basis of the experimental results of temperature and dc bias field dependencies of the dielectric modes. Besides the soft mode observed around the $S_A - S_{C_\alpha}^*$ phase transition, a Goldstone mode was detected in the $S_{C_\alpha}^*$ phase indicating a helicoidal structure with small pitch values. In agreement with a bilayer ordering model, the dielectric absorption in the $S_{C_{FI}}^*$ phase was splitted up into two contributions: one related to a Goldstone mode and the other to an azimuthal antiphase mode.

Résumé. Les mesures diélectriques d'une nouvelle série de cristaux liquides antiferroélectriques présentant diverses séquences de phases sont effectuées dans la gamme de fréquence 10 Hz – 10 MHz. Les propriétés structurales des phases $S_{C_\alpha}^*$ et ferriélectrique $S_{C_{FI}}^*$ sont discutées sur la base des résultats expérimentaux des modes diélectriques en fonction de la température et du champ continu. En supplément du mode mou observé autour de la transition de phase $S_A - S_{C_\alpha}^*$, un mode de Goldstone est détecté dans la phase $S_{C_\alpha}^*$, indiquant ainsi une structure hélicoïdale avec un pas d'hélice très faible. En accord avec un modèle d'arrangement bicouche, l'absorption diélectrique dans la phase $S_{C_{FI}}^*$ se décompose en deux contributions : une liée au mode de Goldstone et l'autre à un mode azimuthal antiphase.

PACS. 77.22-d Dielectric properties of solids and liquids – 77.80-e Ferroelectricity and antiferroelectricity – 77.84-s Dielectric, piezoelectric, and ferroelectric materials

1 Introduction

Antiferroelectricity of chiral smectic liquid crystals was found for the first time in MHPOBC compound [1,2]. Since that time, several hundred antiferroelectric liquid crystals have been synthesized and their properties have been extensively investigated from both theoretical and experimental points of view. Apart from the ferroelectric S_C^* and antiferroelectric $S_{C_A}^*$ phases, these materials may have other tilted subphases such as the $S_{C_\alpha}^*$ phase located just below the S_A phase or the ferroelectric $S_{C_{FI}}^*$ phase intermediate between S_C^* and $S_{C_A}^*$ phases. If the structure of the $S_{C_\alpha}^*$ phase, with molecules in adjacent layers tilted in opposite directions so that the dipoles are cancelled out, is now well established [3], the two other phases mentioned above are still subject of controversy [4–7]. Recently very

promising models for the description of the $S_{C_\alpha}^*$ and $S_{C_{FI}}^*$ phases were proposed.

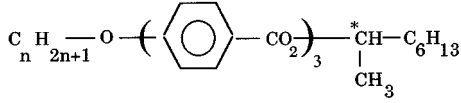
Taking into account a discrete phenomenological model with competing interactions between nearest and next nearest smectic layers, the $S_{C_\alpha}^*$ phase is described as a helicoidally modulated structure similar to the S_C^* phase, except that the pitch is much shorter so that the helix extends over a few layers only [8]. The dielectric response in the $S_{C_\alpha}^*$ phase should therefore consist of the two contributions: the soft mode part and the Goldstone mode part. The soft mode, associated with variations of the molecular tilt angle, is expected to contribute to the dielectric absorption only close to the $S_A - S_{C_\alpha}^*$ phase transition, whereas the Goldstone mode, connected to in-phase fluctuations of the azimuthal angle around the helical axis, should become predominant at lower temperatures in the $S_{C_\alpha}^*$ phase.

As regards the ferroelectric $S_{C_{FI}}^*$ phase, the sequence of phase transition $S_C^* - S_{C_{FI}}^* - S_{C_A}^*$ could be understood employing a simple phenomenological model which assumes a bilayer smectic ordering and an azimuthal reorientation of

^a e-mail: jp.parneix@piom.u-bordeaux.fr

^b UMR CNRS 5501

^c UPR CNRS 8641



n	K	S _{CA} [*]	S _{CFI1} [*]	S _{CFI2} [*]	S _C [*]	S _{Cα} [*]	S _A	I
8	• 89	• (60)	• (72)	• (87,8)	• 94.8	• 95.7	• 141.8	•
9	• 95.8	• (94)	• 96.6	• 100,5	• 108	• 110.5	• 138	•
10	• 90.3	• 102.8	• 104.6	• 106,1	• 116.2	• 117.2	• 138	•
11	• 82.5	• 91.6	• 94.6	• 98.1	• 118.7	-	• 134	•
12	• 69	• 98	• 99.3	• 101	• 121	-	• 130	•

Fig. 1. Molecular formulas and phase sequences of the series under investigation.

the molecules through the transitions [9]. In this model, the tilt angle of the helicoidal structure remains almost constant through the whole S_{CFI}^{*} phase but the difference Ψ in the azimuthal angle in adjacent layers, invariant along the helical axis, changes with the temperature. Consequently a second process may add to the Goldstone mode: the azimuthal antiphase mode related to the fluctuations of the Ψ angle.

In the present work, we report results of dielectric measurements on a family of chiral smectic liquid crystals with emphasis on S_{CA}^{*} and S_{CFI}^{*} phases since the dielectric behaviour in the S_{CA}^{*} phase was analyzed more in detail elsewhere [10].

2 Experimental

We have synthesized an antiferroelectric liquid crystal series [11] ($n = 8 - 12$) having the chemical structure and phase sequence displayed in Figure 1. The phase transition temperatures were obtained by both microscopic observation and DSC. Since the two ferrielectric S_{CFI1}^{*} and S_{CFI2}^{*} phases are distinguished by the sense of their helical twist only, as shown by means of helical pitch measurements in our previous paper [12], they will be considered as a single ferrielectric S_{CFI}^{*} phase in the dielectric study. The dielectric behaviour of the $n = 11, 12$ compounds presenting the direct transition between S_A and S_C^{*} phases without the appearance of the S_{Cα}^{*} phase has already been investigated [12,13]: the following results are rather focused on the $n = 8$ to $n = 10$ compounds.

Sample cells were constructed from two glass substrates with patterned ITO, separated by spacers of 25 μm in thickness and the area of electrodes was 25 mm^2 . Homogeneous alignment was achieved by coating the electrodes with polyimide and rubbing unidirectionnaly. A triangular wave of 4 $\text{V}/\mu\text{m}$, 10 Hz was applied to the sample before

the measurements in order to improve the planar orientation. The alignment was optically controlled using a polarizing microscope with transmitted light. After stabilizing the temperature with an accuracy of 0.05 $^\circ\text{C}$, the complex dielectric constant $\varepsilon^*(f)$ ($\varepsilon^* = \varepsilon' - j\varepsilon''$) was carried out in the frequency range 10 Hz–10 MHz during the cooling run as well as the heating run. The ac measuring voltage was 0.1 V and a dc bias field up to 35 V (14 kV/cm) was applied. A generalized Cole-Cole expression was fitted to the experimental data:

$$\varepsilon^*(f) = \varepsilon_\infty + \sum_i \frac{\Delta\varepsilon_i}{1 + (jf/f_i)^{\alpha_i}}$$

where ε_∞ is the dielectric constant in the high frequency limit, and $\Delta\varepsilon_i$, f_i , α_i are dielectric strength, relaxation frequency and symmetric distribution parameter of the mode (i) respectively.

3 Results and discussion

3.1 S_A – S_C^{*} – S_C^{*} phase sequence

Figure 2 shows the dielectric dispersion curves ε' versus temperature for several frequencies. Similarly to the case of the S_A – S_C^{*} phase transition, the increase of the soft mode contribution to the dielectric response in the S_A phase on approaching the tilted smectic phase is observed. This mode obeys a Curie-Weiss law: the relaxation frequency f_S and the inverse dielectric strength $(\Delta\varepsilon_S)^{-1}$ vary linearly with temperature in the S_A phase. Its contribution to the dielectric constant reaches a maximum at the transition to the S_{Cα}^{*} phase which gives an approximate value of T_c .

Below the phase transition temperature, even if the mode analysis is still carried out as a single mode, we notice a marked increase of the dielectric constant at low frequencies (Fig. 2a) which indicates that the dielectric response becomes slightly polydispersive because both the soft mode and the Goldstone mode may coexist [14]. The fact that we are not able to separate the two contributions originates from the small difference in their relaxation frequencies, since the Goldstone mode occurs in a higher frequency range in the S_{Cα}^{*} phase than in the S_C^{*} one [15]¹. Moreover, under the application of a 35 V bias field, the absorption process is shifted to higher frequencies but the behaviour of its relaxation frequency is qualitatively unchanged as seen in Figure 3, which means that the Goldstone mode contribution is reduced but not completely cancelled out. On the contrary, once in the S_C^{*} phase, this mode is suppressed and only the soft mode remains, its

¹ It should be noted that recent optical studies [16,17,19] have shown the existence of large tilt fluctuations in the vicinity of the S_A – S_{Cα}^{*} phase transition. Such fluctuations can give a contribution in the dielectric response which is difficult to separate from the Goldstone mode contribution. Further dielectric investigations are needed on that point with a better checking of the sample temperature.

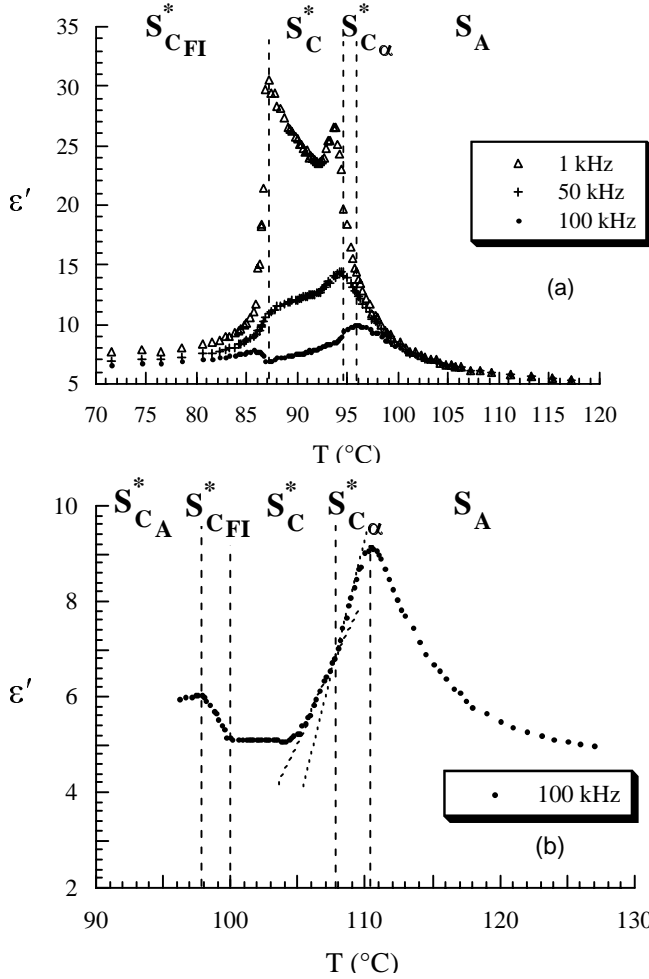


Fig. 2. Temperature dependence of the dielectric dispersion for (a) 1, 50 and 100 kHz ($n = 8$) and (b) 100 kHz ($n = 9$).

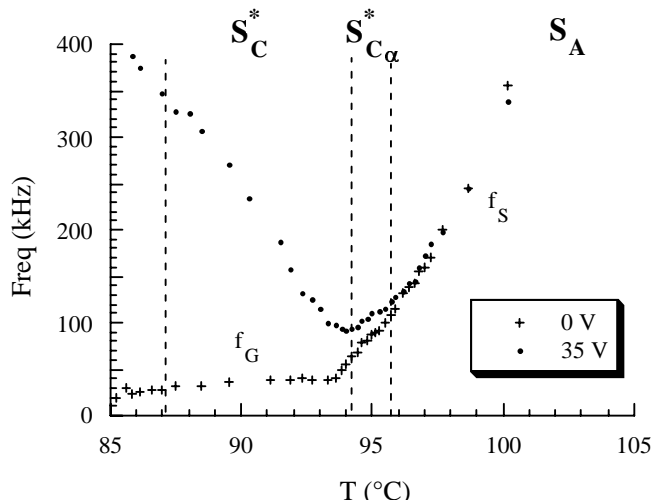


Fig. 3. Bias field influence on the temperature dependence of the relaxation frequency ($n = 8$).

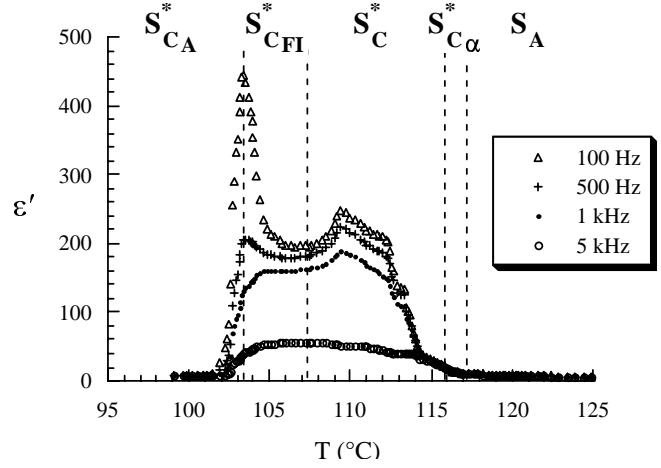


Fig. 4. Temperature dependence of ε' for several frequencies ($n = 10$).

relaxation frequency increasing with decreasing temperature.

Recently, the $S_{C_\alpha}^*$ phase was studied by means of helical pitch measurements: the phase was proved to have a helicoidal structure with very short pitch values of about $0.05 \mu\text{m}$ [20], in agreement with the model developed by Cepic and Zeks [8]. In the same way, the dielectric behaviour depicted above confirms the strong helicoidal twist in the $S_{C_\alpha}^*$ phase. When the helical pitch is small, the relaxation frequency of the Goldstone mode and the threshold bias field for unwinding the helix are expected to be large. This is just what is observed. To conclude with the $S_{C_\alpha}^*$ phase, it should be mentioned that the $S_{C_\alpha}^* - S_C^*$ phase transition is often characterized by a break point on the temperature dependence curve of ε' at high frequencies (Fig. 2b) [21].

3.2 $S_C^* - S_{C_{FI}}^* - S_{C_A}^*$ phase sequence

In the bulk of the ferroelectric S_C^* phase, the dielectric absorption originates in the Goldstone mode whose contribution overwhelms other molecular motions because of its larger dielectric strength. Inside the ferroelectric $S_{C_{FI}}^*$ phase, the Goldstone mode contribution $\Delta\varepsilon_G$ begins to decrease with decreasing temperature since the partial compensation of the local dipole moments occurs. Then at the transition to the antiferroelectric $S_{C_A}^*$ phase, the local polarization cancels out and the dielectric strength of the Goldstone mode vanishes. This reduction of $\Delta\varepsilon_G$ affects the dielectric dispersion and a minimum of the dielectric constant should be observed in the $S_{C_A}^*$ phase. However the most remarkable feature of our experimental results is the occurrence of a sharp peak on $\varepsilon'(T)$ curve at very low frequencies (100 Hz) in the vicinity of the $S_{C_{FI}}^* - S_{C_A}^*$ phase transition (see Fig. 4).

Figure 5 shows the deconvolution of the spectrum in two modes inside the $S_{C_{FI}}^*$ phase. The Goldstone mode appears around 5 kHz and another dielectrically active mode is located between 100 and 200 Hz, more than one decade

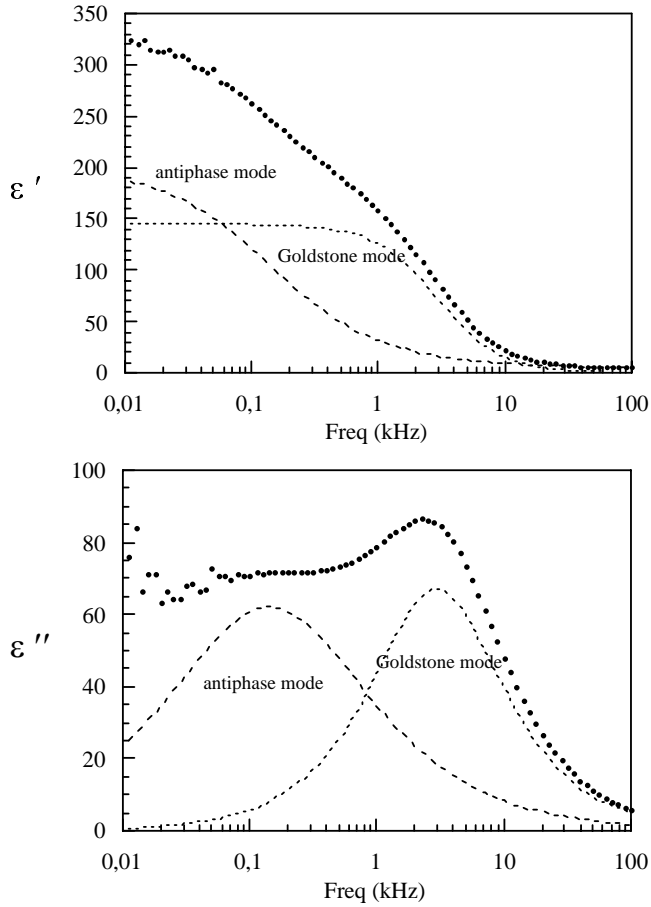


Fig. 5. An example of mode separation in the $S_{C_{FI}}^*$ phase, $T = 104.4^\circ\text{C}$ ($n = 10$).

below the Goldstone mode [21–23]. In the framework of the Lorman's model assuming a bilayer smectic ordering and a constant tilt angle in the whole $S_{C_{FI}}^*$ phase [9], the second mechanism can be understood as the result of fluctuations of the azimuthal antiphase angle Ψ which is related to the azimuthal angle between two adjacent layers, which is equal to $\Psi - 2\pi d/p$, where d is the interlayer distance and p is the helix pitch. $\Psi = 0$ and $\Psi = \Pi$ in the S_C^* and $S_{C_A}^*$ phases respectively and Ψ takes intermediate values in the $S_{C_{FI}}^*$ phase. The amplitude of the associated mode, the so-called azimuthal antiphase mode, is shown to vanish in the ferroelectric phase and to reach a maximum at the $S_{C_{FI}}^* - S_{C_A}^*$ phase transition. We report the temperature dependence of the relaxation characteristics in Figure 6. While the relaxation frequencies f_G and f_a remain almost constant in the $S_{C_{FI}}^*$ phase, the behaviours of the dielectric strengths $\Delta\varepsilon_G$ and $\Delta\varepsilon_a$ radically differ. As expected, $\Delta\varepsilon_G$ decreases with decreasing temperature whereas $\Delta\varepsilon_a$ strongly increases and becomes predominant in the vicinity of the $S_{C_{FI}}^* - S_{C_A}^*$ phase transition so that a marked increase is detected on the dielectric dispersion curve.

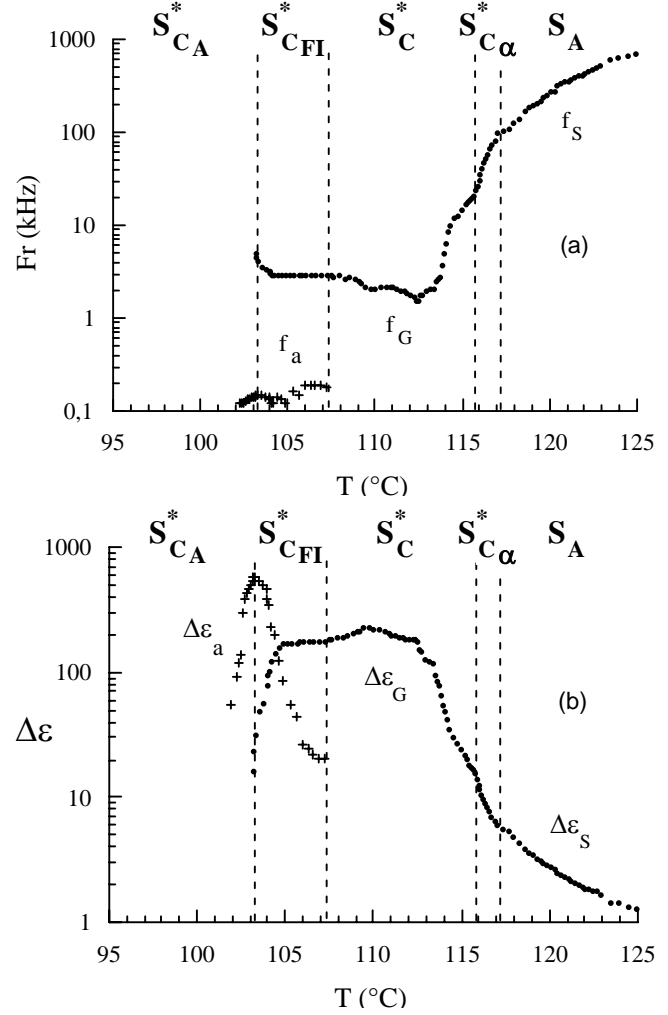


Fig. 6. Temperature dependence of (a) the relaxation frequency f_R and (b) the dielectric strength $\Delta\varepsilon$ ($n = 10$).

4 Conclusion

The effects of bias voltage and temperature on the dielectric properties of an antiferroelectric liquid crystal series have been examined. Both $S_{C_\alpha}^*$ and ferroelectric $S_{C_{FI}}^*$ structures were shown to be helicoidally modulated. On the one hand, a Goldstone mode was detected in the $S_{C_\alpha}^*$ phase with a quite high value of its relaxation frequency indicating that the helix extends over a few layers only. On the other hand, two contributions to the dielectric response were separated in the ferroelectric $S_{C_{FI}}^*$ phase: one related to a Goldstone mode and the other to an azimuthal antiphase mode. The great sensitivity of the ferroelectric $S_{C_{FI}}^*$ phase, and especially of its azimuthal antiphase mode, to the external parameters seems to be a characteristic feature of this phase: the influence of the dc bias field, the anchoring nature and the cell thickness needs to be investigated more in detail.

References

1. A.D.L. Chandani, T. Hagiwara, Y. Suzuki, Y. Ouchi, H. Takezoe, A. Fukuda, *Jpn J. Appl. Phys.* **27**, L729 (1988).
2. A.D.L. Chandani, Y. Ouchi, H. Takezoe, A. Fukuda, K. Terashima, K. Furukawa, A. Kishi, *Jpn J. Appl. Phys.* **28**, L1261 (1989).
3. A.D.L. Chandani, E. Gorecka, Y. Ouchi, H. Takezoe, A. Fukuda, *Jpn J. Appl. Phys.* **28**, L1265 (1989).
4. Y. Takanishi, K. Hiraoka, V.K. Agrawal, H. Takezoe, A. Fukuda, *Jpn J. Appl. Phys.* **30**, 2023 (1991).
5. K. Hiraoka, Y. Takanishi, K. Skarp, H. Takezoe, A. Fukuda, *Jpn J. Appl. Phys.* **30**, L1819 (1991).
6. H. Orihara, Y. Ishibashi, *Jpn J. Appl. Phys.* **29**, L115 (1991).
7. B. Zeks, M. Cepic, *Liq. Cryst.* **14**, 445 (1990).
8. M. Cepic, B. Zeks, *Mol. Cryst. Liq. Cryst.* **263**, 61 (1995).
9. V.L. Lorman, A.A. Bulbitch, P. Tolentino, *Phys. Rev. E.* **49**, 1367 (1994).
10. F. Bibonne, H. Fredon, J.P. Parneix, V. Faye, H.T. Nguyen, *Ferroelectrics* (to be published).
11. V. Faye, J.C. Rouillon, C. Destrade, H.T. Nguyen, *Liq. Cryst.* **19**, 47 (1995).
12. F. Bibonne, J.P. Parneix, N. Isaert, G. Joly, H.T. Nguyen, A. Bouchta, C. Destrade, *Mol. Cryst. Liq. Cryst.* **263**, 27 (1995).
13. J.W. O'Sullivan, J.K. Vij, H.T. Nguyen, *Liq. Cryst.* **23**, 77 (1997).
14. M. Cepic, G. Heppke, J.M. Hollidt, D. Lotzsch, D. Moro, B. Zeks, *Mol. Cryst. Liq. Cryst.* **263**, 207 (1995).
15. G. Chern, H.C. Lin, S.L. Wu, W.J. Hsieh, *J. Appl. Phys.* **79**, 3681 (1996).
16. R. Fahri, H.T. Nguyen, *Europhys. Lett.* **40**, 49 (1997).
17. I. Musevic, M. Skarabot, R. Blinc, W. Schranz, P. Dolinar, *Liq. Cryst.* **20**, 771 (1996); M. Skarabot, I. Musevic, A. Kityk, R. Blinc, 6th Int. Conf. on Ferroelectric Liq. Cryst., Brest, France, Conference Summaries (July, 1997), p. 386.
18. A. Rastegar, I. Musevic, Th. Rasing, 6th Int. Conf. on Ferroelectric Liq. Cryst., Brest, France, Conference Summaries (July, 1997), p. 352.
19. V. Laux, N. Isaert, H.T. Nguyen, P. Cluzeau, C. Destrade, *Ferroelectrics* **179**, 25 (1996).
20. M.R. de la Fuente, S. Merinos, Y. Gonzales, M.A. Perez Jubindo, B. Ros, J.A. Puertolas, M. Castro, *Adv. Matter (Weinheim, Ger.)* **7**, 564 (1995).
21. P. Gisse, J. Pavel, H.T. Nguyen, V.L. Lorman, *Ferroelectrics* **147**, 27 (1993).
22. S. Hiller, S.A. Pikin, W. Haase, J.W. Goodby, I. Nishiyama, *Jpn J. Appl. Phys.* **33**, L1096 (1994).
23. H. Uehara, Y. Hanakai, J. Hatano, S. Saito, K. Murashiro, *Jpn J. Appl. Phys.* **34**, 5424 (1995).